Mon. Not. R. Astron. Soc. **380,** 1053–1063 (2007) doi:10.1111/j.1365-2966.2007.12150.x

Rotational velocities of the giants in symbiotic stars – II. Are S-type symbiotics synchronized?⋆

R. K. Zamanov,[1,2]† M. F. Bode,[2]† C. H. F. Melo,[3,4] R. Bachev,[1] A. Gomboc,[2,5]† I. K. Stateva,[1] J. M. Porter[2] and J. Pritchard[3]

[1]*Institute of Astronomy, Bulgarian Academy of Sciences, 72 Tsarighradsko Shousse Blvd., 1784 Sofia, Bulgaria*
[2]*Astrophysics Research Institute, Liverpool John Moores University, Twelve Quays House, Birkenhead CH41 1LD*
[3]*European Southern Observatory, Casilla 19001, Santiago 19, Chile*
[4]*Departamento de Astronomía, Universidad de Chile, Casilla 36-D, Santiago, Chile*
[5]*Department of Physics, University of Ljubljana, Jadranska 19, 6100 Ljubljana, Slovenia*

Accepted 2007 June 20. Received 2007 June 15; in original form 2007 January 8

ABSTRACT

We have measured the projected rotational velocities ($v \sin i$) of the mass donors for 29 S-type symbiotic stars (SSs) using high-resolution spectroscopic observations and the cross-correlation function (CCF) method. The results of the CCF have been controlled with synthetic spectra. The typical rotational velocity of the K and M giants in S-type symbiotics appeared to be $4.5 < v \sin i < 11.7$ km s^{-1}. In a subsample of 16 S-type SSs (with known orbital periods and well-measured $v \sin i$), 15 have deviations from synchronization less than the 3σ level. This means that we did not find evidence for a statistically significant deviation from the synchronization for any of these 15 objects. The deviation from synchronization is statistically significant (at confidence level >99 per cent) only for the recurrent nova RS Oph.

For 22 S-type symbiotics we give clues as to what their orbital periods could be.

Key words: binaries: symbiotic – stars: late-type – stars: rotation.

1 INTRODUCTION

The symbiotic stars (SSs – thought to comprise a white dwarf (WD) accreting from a cool giant or Mira) represent the extremum of the interacting binary star classification. They offer a laboratory in which to study such important processes as (i) mass-loss from cool giants and the formation of planetary nebulae; (ii) accretion on to compact objects, (iii) photoionization and radiative transfer in gaseous nebulae and (iv) non-relativistic jets and bipolar outflows (e.g. Kenyon 1986; Corradi, Mikolajewska & Mahoney 2003).

On the basis of their infrared properties, SSs have been classified into stellar continuum (S) and dusty (D or D′) types (Allen 1982). The D-type systems contain Mira variables as mass donors. The D′-type are characterized by an earlier spectral type (F-K) of the cool component and lower dust temperatures. All mass donors in D′-type systems appeared to be very fast rotators (see Zamanov et al. 2006, hereafter Paper I).

Our aims here are: (1) to measure the projected rotational velocities ($v \sin i$) and the rotational periods ($P_{\rm rot}$) of the giants in a number of southern S-type SSs, using a cross-correlation function (CCF) approach; (2) to check whether their rotation is synchronized with the orbital period; (3) to provide pointers to the determination of binary periods (assuming corotation).

This is the second in a series of papers exploring the rotation velocities of the mass-donating (cool) components of SSs.

2 OBSERVATIONS

We have observed 30 objects from the Belczyński et al. (2000) SS catalogue and have observed all S-type SSs from the catalogue with $12 < \mathrm{RA} < 24^{\rm h}$, declination $<2^\circ$, and catalogue magnitude brighter than $V < 12.5$.

The observations have been performed with FEROS at the 2.2-m telescope (ESO, La Silla). FEROS is a fibre-fed echelle spectrograph, providing a high resolution of $\lambda/\Delta\lambda = 48\,000$, a wide wavelength coverage from about 4000 to 8900 Å in one exposure and a high throughput (Kaufer et al. 1999). The 39 orders of the echelle spectrum are registered with a 2000×4000 EEV CCD.

The present data have been collected from 2004 April to September. Table 1 gives a log of the observations. All spectra are reduced using the dedicated FEROS data reduction software implemented in the ESO-MIDAS system (www.ls.eso.org/lasilla/sciops/2p2/E2p2M/FEROS/DRS/). A few examples of our spectra are given in Appendix A (Fig. A1).

⋆Based on observations obtained in ESO programmes 073.D-0724A and 074.D-0114.

†E-mail: rkz@astro.bas.bg (RKZ); mfb@astro.livjm.ac.uk (MFB); andreja.gomboc@fmf.uni-lj.si (AG)

Table 1. Journal of observations. The columns are as follows: the name of the object, date of observation (YYYY-MM-DD), the Modified Julian Date (JD − 240 0000.5) of the start of the observation, signal-to-noise ratio (S/N) around λ8500 Å.

Object	Date-obs	MJD-obs	Exposure (s)	S/N
AR Pav	2004-06-04	53160.3737	600	40
AS 255	2004-04-12	53107.3670	1200	45
AS 276	2004-04-12	53107.3967	600	45
AS 289	2004-06-05	53161.3071	600	40
AS 316	2004-06-07	53163.3600	1200	70
AS 327	2004-09-21	53269.0508	600	45
BD-21°3873	2004-04-14	53109.2903	600	80
CD-36°8436	2004-04-11	53106.3374	600	40
CD-43°14304	2004-08-30	53247.2435	1200	70
FG Ser	2004-06-03	53159.2731	1200	50
HD 319167	2004-06-07	53163.3905	600	45
Hen 2−374	2004-06-08	53164.3099	1200	40
Hen 3−1213	2004-04-12	53107.3049	1200	75
Hen 3−1341	2004-04-12	53107.3354	1200	50
Hen 3−1674	2004-06-07	53163.3103	1200	35
Hen 3−1761	2004-06-04	53160.2095	600	40
Hen 3−863	2004-04-11	53106.3067	1200	55
MWC 960	2004-06-08	53164.2738	1200	70
PN Ap 1−9	2004-06-07	53163.1986	1200	45
RS Oph	2004-04-11	53106.3849	600	50
RW Hya	2004-04-12	53107.2285	600	80
SS73 129	2004-06-29	53185.0660	1200	65
SS73 141	2004-06-29	53185.1058	1200	50
V2506 Sgr	2004-06-07	53163.2393	1200	45
V2756 Sgr	2004-06-08	53164.3968	600	40
V2905 Sgr	2004-06-28	53184.0858	1200	90
V3804 Sgr	2004-06-27	53183.9951	1200	40
V4018 Sgr	2004-08-31	53248.1800	1200	50
V4074 Sgr	2004-06-07	53163.2737	600	50
V919 Sgr	2004-06-03	53159.3108	1200	50

3 $v \sin i$ MEASUREMENT TECHNIQUES

3.1 CCF method

The projected rotational velocities have been derived by cross-correlating the observed spectra with K0 numerical masks yielding a CCF whose width ($\sigma_{\rm obs}$) is related to broadening mechanisms such as stellar rotation and turbulence.

The emission lines do have an effect in the CCF and they must be cleaned. They were cut off by fitting a continuum and replacing the emission lines by the value of the fit. Note that the exact location of the continuum is not important.

The numerical K0 mask was constructed from a K0III synthetic spectrum in the region within λλ5000–7000 Å following the procedure described in Baranne, Mayor & Poncet (1979) In the CORAVEL-type cross-correlation a binary mask is used as template instead a real spectrum. This binary (or CORAVEL-type) mask has been used in many different data reduction software for cross-correlation (ELODIE, CORALIE and now HARPS). The K0-mask CCFs for the SSs observed here are plotted in Appendix A (Fig. A2) and $\sigma_{\rm obs}$ are given in Table 2.

In order to use the observed width of the CCF ($\sigma_{\rm obs}$) as an estimate of $v \sin i$ one needs to subtract the amount of broadening contributing to $\sigma_{\rm obs}$ unrelated to the stellar rotation (convection, instrumental profile, etc.), that is, σ_0. For FEROS spectra (see Melo, Pasquini & De Medeiros 2001; Melo 2003):

$$v \sin i = 1.9 \sqrt{\sigma_{\rm obs}^2 - \sigma_0^2}\ {\rm km\,s^{-1}}. \quad (1)$$

More details of the cross-correlation procedure are given in Melo et al. (2001), and also σ_0 is calibrated as a function of the $(B - V)$ for FEROS spectra and for stars with $0.6 < (B - V) < 1.2$. For giants with $(B - V) < 1.2$ in Table 2 as well as in Paper I, the Melo et al. (2001) calibration has been adopted. However, the stars in our sample have $(B - V)$ around 1.5 which is beyond the range of the calibration of Melo et al. (2001). For $(B - V) > 1.2$, we will adopt constant $\sigma_0 = 4.5\,{\rm km\,s^{-1}}$.

This value has been adopted as a result of CCF measurements of few objects with known $v \sin i$, bearing in mind the results of Delfosse et al. (1998). Using a similar template and method but lower resolution (which increases σ_0), Delfosse et al. (1998) have shown that σ_0 does vary over a range of $0.8 < (R - I) < 1.5$ (which corresponds to a spectral type from ∼M0 to ∼M6), decreasing from $\sim 5.1\,{\rm km\,s^{-1}}$ to $4.7\,{\rm km\,s^{-1}}$, bearing in mind the calibration of CCF and FEROS spectra undertaken in Melo et al. (2001).

The errors on CCF $v \sin i$ measurements are dominated by systematic effects rather than by photon noise. The error on $v \sin i$ comes from two main sources: uncertainties on the values of $\sigma_{\rm obs}$ and σ_0. According to error estimate carried out by Melo et al. (2001), stars with $(B - V) < 1.2$ have an error on $v \sin i$ less than $1.2\,{\rm km\,s^{-1}}$. For stars with $(B - V) > 1.2$ we adopt a constant σ_0, which leads to an increase in our errors. For such stars a conservative error of $1.5\,{\rm km\,s^{-1}}$ is assigned. For objects with $v \sin i \geqslant 15\,{\rm km\,s^{-1}}$ the error on $v \sin i$ is ±10 per cent.

In the case of the rapidly rotating Hen 3−1674 the CCF rotation was extracted by a slightly different procedure as described for the fast rotators in Paper I. For V3804 Sgr we did not get a meaningful CCF due to the numerous emission lines in the spectrum at the time of our observations. From measurements of the Fe I 8689 line we obtain a rough estimate of FWHM(Fe I 8689) ≈ 0.58 ± 0.15 Å similar to the width of this line in AR Pav and FG Ser and corresponding to $v \sin i \approx 9 \pm 3\,{\rm km\,s^{-1}}$.

3.2 FWHM method

Besides the cross-correlation procedure another method using full width at half-maximum (FWHM) of spectral lines of observed and synthetic spectra was also applied. This procedure is similar to that described in Fekel (1997). The spectra of K5III ($T_{\rm eff} = 3950$ K, $\log g = 1.5$), M0III ($T_{\rm eff} = 3985$ K, $\log g = 1.2$) and M5III ($T_{\rm eff} = 3424$ K, $\log g = 0.5$) stars have been synthesized by using the code SYNSPEC (Hubeny, Lanz & Jeffery 1994) in the spectral region λ8750–8850 Å.

Local thermodynamic equilibrium model atmospheres were extracted from Kurucz's grid (1993). The VALD atomic line data base (Kupka et al. 1999) was used to create a line list for spectrum synthesis. The value of $3\,{\rm km\,s^{-1}}$ was adopted for the microturbulent velocity. A grid of synthetic spectra for projected rotational velocities from 0 to $60\,{\rm km\,s^{-1}}$ was calculated. The FWHM of a dozen observed spectral lines has been measured and compared to the FWHM of spectral lines from the synthetic spectra. The results are given in the sixth column of Table 2.

The comparison between the CCF and FHWM methods (see Fig. 1) shows that the $v \sin i$ measurements agree well, with typical difference ±(1–2) $\,{\rm km\,s^{-1}}$, as expected from the measurement errors. The only exception is AS 289 (see also Section 6.1).

Table 2. Rotational velocities of the red giants in SSs (measured in this paper). The spectral types are from the catalogue of Belczyński et al. (2000), $(B-V)_0$ is the intrinsic colour (from Schmidt-Kaler 1982) for the corresponding spectral type adopting luminosity class III in all cases, R_g is the adopted radius of the giant [if not otherwise indicated, this is the average radius for the corresponding spectral type taken from table 7 of van Belle et al. (1999)]. P_{orb} is the orbital period (see Section 6). $v \sin i$ (FWHM) is the projected rotational velocity of the cool giant as measured with FWHM method (see Section 3.2). σ_{obs} is the observed width of the CCF. $v \sin i$ is our measurement based on CCF method (see Section 3.1), if other measurements of $v \sin i$ exist, they are also given in the next column. For objects with unknown orbit we give an estimation of the upper limit of the orbital period P_{ul} (i.e. we expect $P_{orb} \lesssim P_{ul}$, see Section 9). The upper part of this table contains objects observed with FEROS; the lower part: $v \sin i$ values are taken from the literature.

Object	Cool spectral type	$(B-V)_0$	R_g $R_\odot$	P_{orb} (d)	$v \sin i$ FWHM (km s^{-1})	σ_{obs} CCF (km s^{-1})	$v \sin i$ CCF (km s^{-1})	Other (km s^{-1})	P_{ul} (d)
AR Pav	M5	1.59	139.6	604.5	8.8 ± 2	6.208	8.1 ± 1.5	11 ± 2^e	–
AS 255	K3	1.26	20.5		9.7 ± 1	6.417	8.7 ± 1.5		119
AS 276	M4.5	1.60	123.0		7.7 ± 2	6.382	8.6 ± 1.5		724
AS 289	M3.5	1.62	89.0	451	9.5 ± 1	8.400	13.5 ± 1.5	5.7 ± 1^k	–
AS 316	M4	1.62	105.5		9.6 ± 1	6.843	9.8 ± 1.5		545
AS 327	M3	1.62	71.5		7.7 ± 1	5.847	7.1 ± 1.5		510
BD-21°3873	K2	1.16	20.8	281.6	6.6 ± 1	5.352	4.6 ± 1.2	5.4 ± 0.7^f	–
CD-36°8436	M5.5	1.58	144.0		6.6 ± 1.5	6.410	8.7 ± 1.5		840
CD-43°14304	K5	1.51	38.8	1448	7.2 ± 1	5.869	7.2 ± 1.5	$<3^g$	–
FG Ser	M5	1.59	139.6	650	9.8 ± 1	6.756	9.6 ± 1.5	$8 \pm 1^h, 7 \pm 1^k$	–
HD 319167	M3	1.62	71.5		7.4 ± 2	6.041	7.7 ± 1.5		472
Hen 2−374	M5.5	1.59	144.0		8.4 ± 1.5	5.712	6.7 ± 1.5		1091
Hen 3−1213	M2/K4	1.54	50:?		9.1 ± 1.5	7.236	10.8 ± 1.5		235
Hen 3−1341	M2	1.61	57.8		7.5 ± 1.5	6.423	8.7 ± 1.5		336
Hen 3−1674	M5	1.59	139.6		56.0 ± 5	–	52.0 ± 5.2		135
Hen 3−1761	M4	1.62	105.5		9.3 ± 2	6.475	8.8 ± 1.5		603
Hen 3−863	K4	1.43	45.0		7.9 ± 1	5.811	7.0 ± 1.5		326
MWC 960	K9	1.55	39.0^a		9.0 ± 1	6.436	8.7 ± 1.5		225
PN Ap 1−9	K4	1.43	45.0		8.2 ± 1	5.792	6.9 ± 1.5		329
RS Oph	M0	1.56	59.1	455.7	13.8 ± 1.5	7.624	11.7 ± 1.5		–
RW Hya	M2	1.61	57.8	370.2	6.2 ± 1	5.837	7.1 ± 1.5	5.0 ± 1^k	–
SS73 129	M0	1.56	59.1		8.9 ± 1	6.162	8.0 ± 1.5		374
SS73 141	M5	1.59	139.6		7.9 ± 1	6.064	7.7 ± 1.5		914
V2506 Sgr	M5.5	1.59	144.0		7.8 ± 1	6.284	8.3 ± 1.5		874
V2756 Sgr	M3	1.62	71.5	243:?	4.2 ± 1.5	4.942	3.9 ± 1.5		932
V2905 Sgr	M5	1.59	139.6		6.6 ± 1	5.708	6.7 ± 1.5		1059
V3804 Sgr	M5	1.59	139.6		9.0 ± 3	–	–		–
V4018 Sgr	M4	1.62	105.5		7.2 ± 1.5	5.345	5.5 ± 1.5		974
V4074 Sgr	M4	1.62	105.5		4.2 ± 1.5	4.871	3.5 ± 1.5		1508
V919 Sgr	M2	1.61	57.8		7.4 ± 1	6.560	9.1 ± 1.5		322
SY Mus	M5		139.6	624.5				7 ± 1^p	
AG Dra	K2Ib or II		$30–40^b$	554				$3.6 \pm 1^k, 5.9 \pm 1^q$	
BX Mon	M5III		139.6	1401				6.8 ± 1^k	
TX CVn	K5III		38.8	199				8.9 ± 1^k	
T CrB	M4IIIelips.		66 ± 11^c	227.57				5.4 ± 1^k	
V443 Her	M5.5III		144	594				4.5 ± 1^k	
CI Cyg	M5II or M5.5		$189–236^d$	854.5				10.4 ± 1^k	
AG Peg	M3III		71.5	817.4				4.5 ± 1^k	
V1329 Cyg	M6		147.9	956.5				7.0 ± 2^k	
BF Cyg	M5III		$75–280^r$	756.8				4.5 ± 2^k	

[a]From the fit in van Belle et al. (1999); [b]Tomov et al. (2000); [c]Belczynski & Mikolajewska (1998) [d]Kenyon & Mikolajewska (1995); [e]Schild et al. (2001); [f]Smith et al. (1997); [g]Schmid et al. (1998); [h]Mürset et al. (2000); [k]Fekel et al. (2003); [p]Schmutz et al. (1994); [q]de Medeiros & Mayor (1999). [r]See Section 6.2.

Because the CCF method uses many more lines and a better defined mathematical procedure, in the analysis we will use $v \sin i$ derived with the CCF method.

4 PARAMETERS OF SYMBIOTIC STARS

4.1 Synchronization in SSs

The physics of tidal synchronization for stars with convective envelopes has been analysed several times (e.g. Zahn 1977, and see the discussion in chapter 8 of Tassoul 2000). There are some differences in the analysis of different authors, leading to varying synchronization time-scales. Here, we use the estimate from Zahn (1977, 1989). The synchronization time-scale in terms of the period is

$$\tau_{syn} \approx 800 \left(\frac{M_g R_g}{L_g} \right)^{1/3} \frac{M_g^2 (M_g/M_2 + 1)^2}{R_g^6} P_{orb}^4 \quad \text{yr}, \qquad (2)$$

where M_g and M_2 are the masses of the giant and WD, respectively, in solar units, and R_g and L_g are the radius and luminosity of the

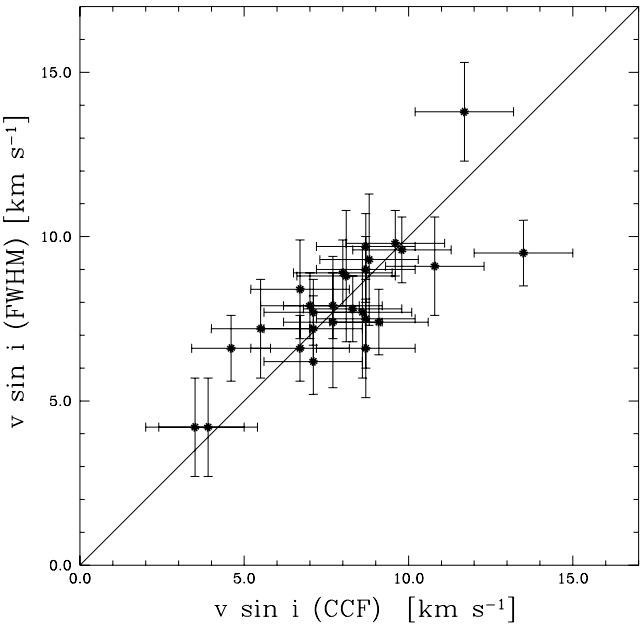

Figure 1. Comparison between the CCF and FWHM measurements of $v \sin i$. The straight line indicates $v \sin i$ (CCF) = $v \sin i$ (FWHM).

giant, also in solar units. The orbital period $P_{\rm orb}$ is measured in days.

In Table 3 we calculate this time-scale for a few representative cases. We point out that these values serve as an estimation. From the $R_{\rm g}^6$ dependence of $\tau_{\rm syn}$ in equation (1), one can expect large uncertainties in the synchronization time-scale as a result of the uncertainties in the red giant radius. There is also a $P_{\rm orb}^4$ dependence, which can introduce large uncertainties, but $P_{\rm orb}$ is much more accurately known than $R_{\rm g}$.

As can be seen in Table 3, for S-type SSs depending on the binary parameters, $\tau_{\rm syn}$ can be as short as $<10^4$ yr and longer than 10^7 yr. Short $\tau_{\rm syn}$ can be expected when the radius of the mass donor is a significant fraction of the orbital separation.

The lifetime of the symbiotic phase for a red giant or asymptotic giant branch star is around 10^5 yr (see e.g. Yungelson et al. 1995), which is comparable with $\tau_{\rm syn}$.

4.2 Inclination

In our calculations, we assume that the rotational axis of the red giant is perpendicular to the orbital plane (see Fekel 1981; Hale 1994; Stawikowski 1994). To calculate the rotational periods of the mass donors ($P_{\rm rot}$) we need to know the inclination of the orbit (i) and $R_{\rm g}$.

For eclipsing binaries we can adopt inclination $i = 70^\circ - 110^\circ$, which produces small errors in $\sin i$. For such cases we will assume that $\sin i$ is in the range 0.94–1.00. For other cases we use results from spectropolarimetric observations or radial velocity measurements.

Table 3. The synchronization time, $\tau_{\rm syn}$, calculated following equation (1) for a few representative cases. The typical values for $L_{\rm g}$ and $R_{\rm g}$ of K5III and M4III stars are adopted following van Belle et al.(1999).

Mass donor spectral type	$L_{\rm g}$ ($L_\odot$)	$M_{\rm g}$ ($M_\odot$)	$R_{\rm g}$ ($R_\odot$)	$P_{\rm orb}$ (d)	M_2 ($M_\odot$)	$\tau_{\rm syn}$ (yr)
K5III	350	2	40	200	1.0	7000
				1500	1.0	2.10^7
M4III	1380	1	105	500	0.5	140
		2		500	1.0	700
		3		500	1.0	3200
		2		1500	1.0	60 000

Table 4. Stellar radii of M giants. In column 3 are given $R_{\rm g}$ (following van Belle et al. 1999), in column 4 – mass of the M giants (from Mikolajewska (2003), in column 5 – the range of $R_{\rm g}$ for the corresponding mass and spectral type (following Dumm & Schild 1998).

Object	Mass donor	$R_{\rm g}$ ($R_\odot$)	$M_{\rm g}$ ($M_\odot$)	$R_{\rm g}$ ($R_\odot$)
1	2	3	4	5
FG Ser	M5III	140	1.7	110–150
AR Pav	M5III	140	2.5	90–240
AG Peg	M3III	72	>1.8	60–90
BX Mon	M5III	140	3–3.7	150–200
SY Mus	M5III	140	1.3	60–100
RW Hya	M2III	58	1.6	40–80
AR Pav	M5III	140	2.5–3	130–160
BF Cyg	M5III	140	1.8	110–140
AG Peg	M3III	72	$\gtrsim$1.8	60–90

4.3 Radius of the cool component

For a few objects, the radii of the cool components are derived from model calculations. If the radius of the giant ($R_{\rm g}$) is not known, we will use the average radius for the corresponding spectral type taken from van Belle et al. (1999), always adopting luminosity class III and error ± 5per cent.

For the M giants these values are similar to the stellar radii of M giants in the *Hipparcos* catalogue as calculated by Dumm & Schild (1998). Dumm & Schild (1998) have also shown that the radius of the M giants depends on the mass. For nine objects included in our sample, the masses of the M giants are listed in Mikolajewska (2003). In Table 4, we compare the values adopted here (following van Belle et al. 1999) with the results of Dumm & Schild (1998).

As visible in most cases, the adopted radii (following van Belle et al. 1999) are in agreement with the mass-dependent radii of Dumm & Schild (1998). There are two cases where the adopted values are outside of this range: BX Mon and SY Mus (see Section 6).

5 RESULTS

Our measurements of $v \sin i$ together with data collected from the literature are summarized in Table 2. Our sample thus contains 39 objects (29 with $v \sin i$ measured by us and 10 taken from the literature). This sample should have no biases in the rotational speed of the cool giant, even though the sample is flux limited.

In our sample of S-type SSs, the projected rotational velocities of the mass donors are from 3.5 up to 52 km s^{-1}. Including our data and the data from the literature, we obtain for $v \sin i$: mean = 8.7 km s^{-1}, median = 7.7 km s^{-1}, standard deviation = 7.4 km s^{-1}.

If we exclude the two slowest and the two fastest rotators we get: mean $v \sin i = 7.6 \pm 1.8$ km s^{-1}. In effect, 90 per cent of the mass donors in S-type SSs with measured rotation have $v \sin i$ in the interval $4.5 \leqslant v \sin i \leqslant 11.7$ km s^{-1}. For the southern S-type

symbiotics (29 objects, flux-limited sample, FEROS observations) the values are similar: median $v \sin i = 8.1$ km s^{-1}, 90 per cent of the objects in the interval $4 \leqslant v \sin i \leqslant 11.7$ km s^{-1}.

6 S-TYPE SYMBIOTICS WITH KNOWN ORBITAL PERIODS

In our sample, there are 17 objects with known orbital periods and one where this is inferred (V2756 Sgr). In this section we compare the orbital periods with the rotational periods of the mass donors object by object. The upper–lower limits of $P_{\rm rot}$ are calculated from

$$P_{\rm rot} = \frac{2\pi(R_{\rm g} \pm e_1)(\sin i \pm e_2)}{v \ \sin i \mp e_3}, \quad (3)$$

where e_1, e_2 and e_3 are the corresponding errors in $R_{\rm g}$, $\sin i$ and $v \sin i$, respectively.

In the statistical analysis (Section 8), for $P_{\rm rot}$ we will use the average value between these upper–lower limits and will consider them as corresponding to $\pm 1\sigma$ error.

6.1 Objects with known orbital periods observed by us

AR Pav: It is an eclipsing binary with $P_{\rm orb} \approx 604.5$ d (Bruch, Niehues & Jones 1994). The giant's radius derived from the eclipse is $R_{\rm g} = 137 \pm 20\,{\rm R}_\odot$ (Quiroga et al. 2002), which is very close to the value adopted in Table 2 from the spectral type of the cool giant and to $R_{\rm g} = 139 \pm 10\,{\rm R}_\odot$ (Skopal 2005). We calculate $649 < P_{\rm rot} < 1120$ d.

AS 289 (V343 Ser): It has orbital period $P_{\rm orb} = 450.5 \pm 2.2$ d, $e = 0.135 \pm 0.046$, and orbital inclination of 17°–23° (Fekel et al. 2001). Kenyon & Fernandez-Castro (1987) gave spectral type M3.9III, but more recently M3.5 is assigned from Mürset & Schmid (1999). Assuming it is a normal M3.5III star, and using our CCF value for $v \sin i$, we obtain $159 < P_{\rm rot} < 341$ d.

In a binary with an eccentric orbit the synchronization is reached at a value of $P_{\rm rot} < P_{\rm orb}$ (pseudo-synchronization, see Hut 1981). Following equations (42) and 43 of Hut (1981), in AS 289 the pseudo-synchronization is expected at $P_{\rm rot} = 0.90\,P_{\rm orb}$.

It is worth noting that Fekel et al. (2004) give a value of $v \sin i = 5.7 \pm 1$ km s^{-1} and our FWHM method give $v \sin i = 9.5 \pm 1$ km s^{-1}. An independent measurement of $v \sin i$ with better spectroscopic resolution will be valuable.

BD-21°3873: It has $P_{\rm orb} = 281.6 \pm 1.2$ d, $\sin i = 0.87$ (Smith et al. 1997). We derive $147 < P_{\rm rot} < 293$ d. The object is thus synchronized within the measurement errors.

RW Hya: It is an eclipsing binary with $P_{\rm orb} = 370.4 \pm 0.8$ d (Schild, Muerset & Schmutz 1996). Supposing $i = 70^\circ$–90°, we calculate that $P_{\rm rot}$ is in the interval 301–552 d. The object is thus synchronized within the measurement errors.

FG Ser (AS 296): It is an eclipsing binary with $P_{\rm orb} = 650 \pm 5$ d (Mürset et al. 2000). Supposing $i = 70^\circ$–90°, we calculate $P_{\rm rot} \approx 563$–918 d. The object is thus synchronized within the measurement errors.

6.2 Objects with known periods, not observed by us

Fekel, Hinkle & Joyce (2004) published values of $v \sin i$ for 13 S-type SSs. In this section, if not otherwise stated, we use their measurements.

SY Mus: It is an eclipsing binary with $i = 95\overset{\circ}{.}8 \pm 1\overset{\circ}{.}7$ (Harries & Howarth 1996, 2000), $P_{\rm orb} = 624.5$ d and $v \sin i = 7 \pm 1$ km s^{-1} (Schmutz et al. 1994; Kenyon & Mikolajewska 1995; Pereira, Vogel & Nussbaumer 1995). We calculate $P_{\rm rot} \approx 830$–1230 d. [If we use $R_{\rm g} \approx 80\,{\rm R}_\odot$ (see Section 4.3), we get $P_{\rm rot} \approx 480$–705 d, a range which includes the orbital period.]

AG Dra: It is a yellow SS with spectroscopic $P_{\rm orb} = 548.5 \pm 2$ d (Fekel et al. 2000b; Friedjung et al. 2003), and $i \approx 30^\circ$–45° (Mikolajewska et al. 1995). The cool component is a K2 Ib or II (Zhu et al. 1999). There are two measurements of $v \sin i$: 5.9 ± 1.0 km s^{-1} (de Medeiros & Mayor 1999) and 3.6 ± 1.0 km s^{-1} (Fekel et al. 2004). We adopt $v \sin i = 4.8 \pm 1.0$ km s^{-1}. Skopal (2005) calculated $R_{\rm g} = 33 \pm 11\,{\rm R}_\odot$. Following Tomov, Tomova & Ivanova (2000) and the references therein we can adopt $R_{\rm g} = 30$–$40\,{\rm R}_\odot$. We then estimate $P_{\rm rot} \approx 130$–485 d.

TX CVn: It has $P_{\rm orb} = 199 \pm 3$ d, $e = 0.16 \pm 0.06$, with the cool component a normal K5III star, and inclination $20^\circ < i < 70^\circ$ (Kenyon & Garcia 1989). The luminosity class could also be II or Ib (Zhu et al. 1999). We calculate $P_{\rm rot} \approx 64$–242 d. Pseudo-synchronization (see Hut 1981) is expected at $P_{\rm rot} = 0.87 P_{\rm orb}$. The object is thus (pseudo)-synchronized within the measurement errors.

AG Peg: It has $P_{\rm orb} = 818.2 \pm 1.6$ d and $e = 0.110 \pm 0.039$ (Fekel et al. 2000a), normal M3III and $i \sim 40^\circ$–60° (Kenyon et al. 1993). We calculate $P_{\rm rot} \approx 400$–933 d. The object is thus synchronized within the measurement errors.

V1329 Cyg: It has $P_{\rm orb} = 963.1 \pm 9.8$ d (Chochol & Wilson 2001) and inclination $i = 86^\circ \pm 2^\circ$ (Schild & Schmid 1997). We calculate $P_{\rm rot} \approx 734$–1571 d. The object is thus synchronized within the measurement errors.

T CrB: It has $P_{\rm orb} = 227.57$ d (Fekel et al. 2000a), and $R_{\rm g} = 66 \pm 11\,{\rm R}_\odot$ (Belczynski & Mikolajewska 1998). [It should be noted that Skopal (2005) gives $R_{\rm g} = 75 \pm 12(d/960\,{\rm pc})$, and that a normal M4III would have $R_{\rm g} \approx 105.5\,{\rm R}_\odot$.] The inclination of the system is $i \approx 65^\circ$–70° (Stanishev et al. 2004).

We calculate $P_{\rm rot} \approx 391$–832 d, which differs from the expectations for synchronization. This result is unexpected; however, it appears that this deviation is not statistically significant (see Table 5). From equation (1) we get $\tau_{\rm syn} < 100$ yr. The red giant in

Table 5. The deviations of the individual objects from the line $P_{\rm rot} = P_{\rm orb}$. In the second column the deviations are given in units of σ, where σ is the individual error of $P_{\rm rot}$. The third column gives the probability for random deviation. To reject the null hypothesis (synchronization) at 99 per cent confidence level, $p(\chi^2)$ has to be smaller than 0.01.

Object	Deviation (σ)	$p(\chi^2)$
SY Mus	2.2	0.026
AG Dra	1.4	0.175
BX Mon	1.2	0.223
TX CVn	0.5	0.605
T CrB	1.7	0.082
V443 Her	0.8	0.423
CI Cyg	0.7	0.489
AG Peg	0.6	0.569
V1329 Cyg	0.5	0.651
BF Cyg	0.9	0.361
AR Pav	1.2	0.233
V343 Ser	2.2	0.028
BD-21°3873	0.8	0.399
CD-43°14304	15.9	$<10^{-6}$
FG Ser	0.5	0.610
RS Oph	6.7	$<10^{-6}$
RW Hya	0.4	0.655

T CrB is ellipsoidally shaped (Yudin & Munari 1993). This means that the object has to be synchronized.

BX Mon: The orbital parameters of this eclipsing system are: $P_{\rm orb} = 1401$ d, eccentricity $e = 0.49$ (Dumm et al. 1998); $P_{\rm orb} = 1259$ d, $e = 0.44$ (Fekel et al. 2000a).

We calculate $P_{\rm rot} \approx 800-1278$ d [if we use $R_{\rm g} \approx 170\,{\rm R}_{\odot}$ (see Section 4.3), we get $P_{\rm rot} \approx 970-1550$ d]. BX Mon is the only SS with considerable orbital eccentricity in our sample. SSs with $P_{\rm orb} >$ 800 d tend to eccentric orbits (Fekel et al. 2007). In a binary with $e = 0.44$, the pseudo-synchronization is expected at about $P_{\rm rot} = 0.46\,P_{\rm orb}$ (see Hut 1981).

The time-scale for synchronization in SSs is ∼10 times shorter then the circularization time (see Schmutz et al. 1994). All this implies that in this system the red giant is more or less (pseudo)-synchronized, but the orbit is not circularized yet. It has therefore to be in the process of circularization.

V443 Her: It is not eclipsing, with $P_{\rm orb} = 599.4 \pm 2.1$ d (Fekel et al. 2000b), viewed at an inclination $i \sim 30^{\circ}$ (Dobrzycka et al. 1993). We calculate $P_{\rm rot} = 528-1245$ d. The red giant is thus synchronized within the measurement errors.

CI Cyg: It is an eclipsing binary with orbital period 855.6 d and orbital separation $a = 2.2$ au (Kenyon et al. 1995). Kenyon et al. (1995) have shown that the mass donor is an M5II asymptotic branch giant, filling its tidal surface. They calculated from the eclipse that $R_{\rm g}/a \sim 0.4-0.5$ which means that $R_{\rm g} \approx 189-236\,{\rm R}_{\odot}$. We calculate $P_{\rm rot} = 780-1270$ d. The object is thus synchronized within the measurement errors.

BF Cyg: It is an eclipsing binary with $P_{\rm orb} = 757.3$ d and inclination $i \approx 70-90^{\circ}$ (Pucinskas 1970; Skopal et al. 1997). If the cool component is a normal M5III giant we expect $R_{\rm g} = 139.6 \pm 5$ per cent ${\rm R}_{\odot}$. Mikolajewska, Mikolajewski & Kenyon (1989) suggested $R_{\rm g} \sim 75\,{\rm R}_{\odot}$; however, Skopal et al. (1997) give $R_{\rm g} = 260 \pm 20\,{\rm R}_{\odot}$. Using $v \sin i = 4.5 \pm 2$ km s^{-1}, we calculate $P_{\rm rot} \sim 560-5660$ d.

There are signs that the red giant is ellipsoidally shaped (Yudin et al. 2005). $\tau_{\rm syn}$ for such an object will be short, from equation (1) we get $\tau_{\rm syn} < 7000$ yr. It means that the red giant has to be tidally locked and most probably the $R_{\rm g}$ is closer to a value $\sim 75\,{\rm R}_{\odot}$.

7 QUESTIONABLE OBJECTS

RS Oph: It has orbital period $P_{\rm orb} = 455.72 \pm 0.83$ d (Fekel et al. 2000a). The inclination is about 30°–40° (Dobrzycka & Kenyon 1994; Dobrzycka et al. 1996). This will give a $108 < P_{\rm rot} < 197$ d, that is, 2–3 times less than the orbital period.

RS Oph is a peculiar SS exhibiting different types of activity – recurrent nova eruptions, jet or blob ejections, flickering (see Bode et al. 2006, and references therein).

This is one of the two objects in our sample whose deviation from synchronization is statistically significant (at confidence level >99 per cent, see Table 5). The red giant in RS Oph seems to rotate faster than the orbital period, which means that it has to be in a process of deceleration (the expected $\tau_{\rm syn} \leqslant 5.10^4$ yr).

While there are no doubts about $P_{\rm orb}$, any of the other parameters ($v \sin i$, inclination, red giant radius) have to be checked with independent measurements.

It is noteworthy that our experiments to measure $v \sin i$ with CCF and spectra from different epochs showed that $v \sin i$ could even be higher (up to 14.5 ± 1.5 km s^{-1}).

CD-43°14304: Schmid et al. (1998) reported a circular orbit, $P_{\rm orb} = 1448 \pm 100$ d. They argued that the presence of phase-dependent Hα variations is attributable to occultation effects, suggesting a relatively high inclination, $i > 45^{\circ}$. Spectropolarimetry (Harries & Howarth 2000) gives two possible values for the inclination of the system $i = 57^{\circ} \pm 5^{\circ}$ or $122^{\circ} \pm 48^{\circ}$. The second corresponds to an improbably large eccentricity for the orbit. Therefore we can accept $\sin i = 0.79 - 0.88$. With our value of $v \sin i$ we calculate $P_{\rm rot} \approx 170 - 321$ d.

However, Schmid et al. (1998) found no evidence for rotational broadening in the cool-giant spectrum and were able to place an upper limit on $v \sin i < 3$ km s^{-1}. We measured $v \sin i = 7.2 \pm 1.5$ km s^{-1}; the CCF looks good (see Fig. A2) and FWHM method gives a similar result. If our CCF result is wrong and that of Schmid et al. (1998) is a correct one, then the object is probably synchronized. To avoid confusion we will exclude this star from the analysis, but an independent check of $v \sin i$ would be valuable.

V2756 Sgr (Hen 2−370, SS73 145): The parameters of the system are not well known. We calculate $P_{\rm rot} < 1595$ d. A photometric period of 243 d is supposed in Hoffleit (1970). This photometric period is not confirmed with radial velocity measurements to be that of the orbit. If this is the orbital period and the red giant is tidally locked, then the inclination of the system would be about $i \sim 15^{\circ}$.

Hen 3−1674: It is the fastest rotator in our sample. The catalogues indicate that the mass donor is probably M5III star (see Table 2 and the references therein). A normal M5III star would have $R_{\rm g} \approx 90 - 160\,{\rm R}_{\odot}$ (van Belle et al. 1999) and $M_{\rm g} \approx 1-3\,{\rm M}_{\odot}$, which means a break-up velocity of 30–60 km s^{-1}. If our measurements and the adopted parameters of the system are correct then Hen 3−1674 rotates close to its critical velocity and has rotation similar to that of D′-type SSs (see Paper I).

8 ARE THE MASS DONORS IN S-TYPE SYMBIOTICS SYNCHRONIZED (COROTATING)?

Fig. 2 shows the rotational period versus the orbital period of the 17 objects in our sample, with a straight line indicating the corotation (i.e. $P_{\rm rot} = P_{\rm orb}$). Most objects are close to this line, which suggests that they are synchronized. In Table 5 are given the individual deviations as well as the corresponding probability that the deviation is random. Nine objects are synchronized within the measurement errors (1σ level). Four objects have deviations between 1 and 2σ. Generally, 15 out of 17 are within the 3σ level. The two objects that are outside of the 3σ level are RS Oph and CD-43°14304.

The standard χ^2 test gives a probability of $p(\chi^2) < 10^{-6}$ that the corotation straight line fits the data points when we use all 17 objects. Here we have considered the errors of the rotational period only, the errors of $P_{\rm orb}$ are supposed to be small (usually they are <2 per cent). The straight line cannot be rejected as a fit to the data at more than 90 per cent confidence level, $p(\chi^2) = 0.127$, when the two deviating objects (CD-43°14304 and RS Oph) are excluded. The χ^2 statistic tests how well the data are described by the model, assuming that all the deviations are due to measurement errors and not to intrinsic scatter.

When intrinsic scatter is allowed, as we expect it to be the more realistic situation, one can apply the weighted least-squares estimator (e.g. Akritas & Bershady 1996) to find the slope (β) and the intercept (α) of a linear fit in the form $P_{\rm rot} = \alpha + \beta P_{\rm orb}$ to the data points with measurement errors and non-negligible intrinsic scatter. When all objects are included, we get $\alpha = 204 \pm 49$ and $\beta = 0.14 \pm 0.07$, which is not consistent with $P_{\rm rot} = P_{\rm orb} (\alpha = 0, \beta = 1.0)$. The situation changes if CD-43°14304 is removed from the sample, then $\alpha = -110 \pm 77$ and $\beta = 0.93 \pm 0.16$. When the deviating recurrent

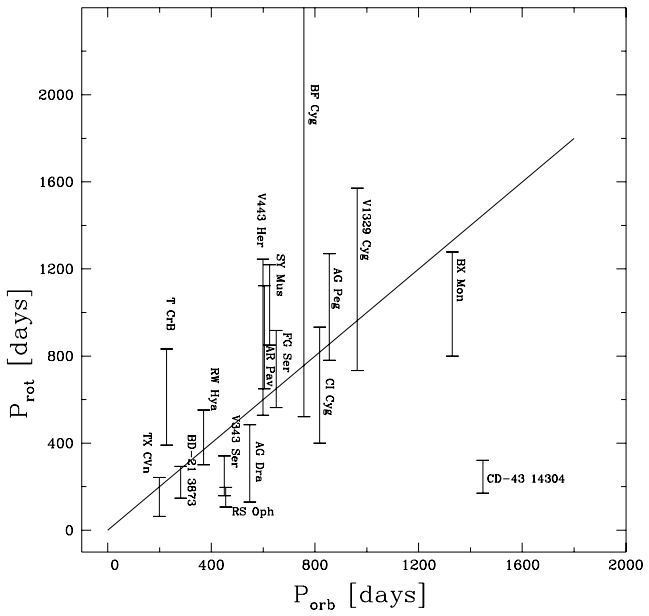

Figure 2. The rotational period of the red giant ($P_{\rm rot}$) versus the orbital period ($P_{\rm orb}$) of the 17 objects in our sample. The solid line corresponds to $P_{\rm rot} = P_{\rm orb}$. Most objects are close to this line, which indicates that they are synchronized. There are two objects which deviate considerably from that rule (RS Oph and CD-43°14304).

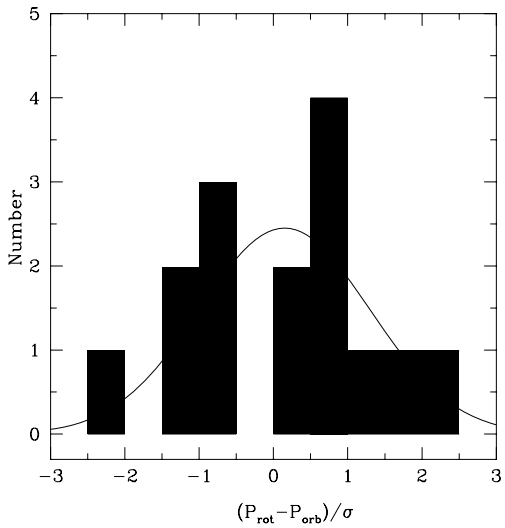

Figure 3. The distribution of $(P_{\rm rot} - P_{\rm orb})/\sigma$ for 15 SSs and the fitted Gaussian (σ is the error of $P_{\rm rot}$). The KS statistic gives only a 38 per cent probability that the parent distribution deviates from the normal one (not statistically significant).

nova RS Oph is removed as well, we obtain $\alpha = -32 \pm 78$ and $\beta = 1.01 \pm 0.17$. The last result is fully consistent with $P_{\rm orb} = P_{\rm rot}$ line ($\alpha = 0$, $\beta = 1$).

Although the synchronization line seems to fit well the data, we still cannot rule out the possibility that one or more outlying objects may determine a false correlation between the variables. Therefore, a rank-correlation test appears appropriate. The Spearman rank-correlation coefficient between the two periods is 0.61 when all 17 objects were included, and about 0.82 for 16 and 15 objects only. This result implies a significant correlation between the variables, since the p-values are less than 0.02 and 0.002, respectively. The similar Kendall-tau test gives similar results, with p-values less than 0.01 for all cases.

The objects that deviate significantly from the $P_{\rm orb} = P_{\rm rot}$ line are RS Oph (a peculiar SS as noted above) and CD-43°14304 (with possible error in the $v \sin i$ measurement, see Section 7). Taking into account the uncertainties of their $P_{\rm rot}$, one finds that the probabilities for a random deviation are less than 0.01 for them (see Table 5), while for all the other 15 stars this idea cannot be rejected at the 0.01 significance level. In other words the null hypothesis that all S-type SSs with well measured $v \sin i$ are synchronized (excluding RS Oph and CD-43°14304) cannot be rejected at the 99 per cent confidence level.

An additional test that may give some clues about the extent of synchronization of the periods is the Kolmogorov–Smirnov (KS) test of how much $(P_{\rm rot} - P_{\rm orb})/\sigma$ deviates from the normal distribution. Even when all 17 stars are included, the p-value of the KS statistics is slightly less than 10 per cent. When only the above 15 objects are included (see Fig. 3), the distribution becomes much narrower (mean = 0.15, $\sigma = 1.23$, KS statistics is 0.38), with a standard deviation comparable to the measurement errors of $P_{\rm rot}$, $< \sigma/P_{\rm rot} > = 0.53$. This means that the hypothesis that the sample comes from a normal distribution cannot be rejected statistically.

We see that the null hypothesis for synchronization of the red giants in SSs cannot be rejected statistically (except probably for RS Oph).

9 CLUES TO THE ORBITAL PERIODS

Up to now, out of 188 SSs, the orbital elements and binary periods are well known for ∼40 objects only (and they are all S-type objects). The derived orbital periods are in the range 200–2000 d (Mikolajewska 2003).

Because the orbital periods of the majority of SSs are unknown, an indirect method to obtain $P_{\rm orb}$ is to measure $v \sin i$. If the mass donors in SSs are corotating ($P_{\rm rot} = P_{\rm orb}$), we can find clues for the orbital periods via the simple relation $P_{\rm orb}\, v_{\rm rot} = 2\pi\, R_{\rm g}$, where $P_{\rm orb}$ is the orbital period, $v_{\rm rot}$ and $R_{\rm g}$ are the rotational velocity and radius of the giant, respectively. The underlying suppositions are: (1) corotation (see Section 8) and (2) rotational axis of the red giant perpendicular to the orbital plane (see Section 4.2 and references therein).

It could be useful in the case of eclipsing binaries, where $\sin i \approx 1$ and $v \sin i \approx v_{\rm rot}$; however, in such cases it is easy to find $P_{\rm orb}$ with photometry. If the inclination is unknown, we can only put an upper limit, $P_{\rm orb} \lesssim P_{\rm ul}$, where $P_{\rm ul} = 2\pi\, R_{\rm g}/\, v \sin i$. To see how useful this predictor is, we calculated the upper limits for the objects with known orbital periods, and we get $P_{\rm ul}/P_{\rm orb} \sim 0.5{-}1.5$.

For the objects with unknown periods, the upper limits for $P_{\rm orb}$ calculated in this way are given in the last column of Table 2. These upper limits are in the interval 100–1500 d. Most of them are similar to those of the measured orbital periods in S-type SSs. However, it seems that for AS 255 and Hen 3−1674, $P_{\rm orb}$ could be as short as $\lesssim$150 d.

10 CONCLUSIONS

We have observed 30 S-type SSs with the FEROS spectrograph. We have measured the rotational velocities of the mass donors for 29 of them by the means of the CCF method (for V3804 Sgr we did not get a meaningful CCF). The results of the CCF method have been checked by the FWHM measurements. The main results are as follows.

(i) The projected, rotational velocities of the cool components in S-type SSs are from 3.5 km s^{-1} up to 52 km s^{-1} and 90 per cent of them are in the interval from 4.5 to 11.7 km s^{-1}.

(ii) In our sample of 17 S-type SSs with known orbital periods, nine are synchronized within the measurement errors (1σ level). If we exclude the doubtful object CD-43°14304 and the recurrent nova RS Oph, all remaining 15 objects are synchronized within the 3σ level. In other words, the null hypothesis that these 15 objects are synchronized can not be rejected statistically at the 99 per cent confidence level.

(iii) Among all objects with $v \sin i$ measured by us the deviation from synchronization is statistically significant (at the 99 per cent confidence level) only for RS Oph. The red giant in this peculiar object seems to rotate faster than the orbital period.

(iv) For 22 S-type SSs with unknown parameters, we give clues as to what their orbital periods could be.

In future it will be interesting: (i) to measure the projected rotational velocity of the cool giants in more SSs; (ii) to compare their rotational velocity with that of the isolated giants and those in other binary systems.

ACKNOWLEDGMENTS

This research has made use of SIMBAD, IRAF and Starlink. RKZ was supported by a PPARC Research Assistantship and MFB was a PPARC Senior Fellow. AG acknowledges the receipt of Marie Curie Fellowship and Marie Curie European Re-integration Grant from the European Commission. This work was partially complete when Dr John Porter passed away in 2005 June and we dedicate this paper to his memory.

REFERENCES

Allen D. A., 1982, in Friedjung M., Viotti R., eds, Proc. IAU Coll. 70, The Nature of Symbiotic Stars. Reidel, Dordrecht, p. 27
Akritas M. G., Bershady M. A., 1996, ApJ, 470, 706
Baranne A., Mayor M., Poncet J. L., 1979, Vistas Astron., 23, 279
Belczynski K., Mikolajewska J., 1998, MNRAS, 296, 77
Belczyński K., Mikolajewska J., Munari U., Ivison R. J., Friedjung M., 2000, A&AS, 146, 407
Bode M. F., O'Brien T. J., Osborne J. P. et al., 2006, ApJ, 652, 629
Bruch A., Niehues M., Jones A. F., 1994, A&A, 287, 829
Chochol D., Wilson R. E., 2001, MNRAS, 326, 437
Corradi R. L. M., Mikolajewska J., Mahoney T. J., eds, 2003, ASP Conf. Ser. Vol. 303, Symbiotic Stars Probing Stellar Evolution. Astron. Soc. Pac., San Francisco, p. 303
de Medeiros J. R., Mayor M., 1999, A&AS, 139, 433
Delfosse X., Forveille T., Perrier C., Mayor M., 1998, A&A, 331, 581
Dobrzycka D., Kenyon S. J., Mikolajewska J., 1993, AJ, 106, 284
Dobrzycka D., Kenyon S. J., 1994, AJ, 108, 2259
Dobrzycka D., Kenyon S. J., Proga D., Mikolajewska J., Wade R. A., 1996, AJ, 111, 2090
Dumm T., Schild H., 1998, New Astron., 3, 137
Dumm T., Muerset U., Nussbaumer H., Schild H., Schmid H. M., Schmutz W., Shore S. N., 1998, A&A, 336, 637
Fekel F. C. Jr, 1981, ApJ, 246, 879
Fekel F. C., 1997, PASP, 109, 514
Fekel F. C., Joyce R. R., Hinkle K. H., Skrutskie M. F., 2000a, AJ, 119, 1375
Fekel F. C., Hinkle K. H., Joyce R. R., Skrutskie M. F., 2000b, AJ, 120, 3255
Fekel F. C., Hinkle K. H., Joyce R. R., Skrutskie M. F., 2001, AJ, 121, 2219
Fekel F. C., Hinkle K. H., Joyce R. R., 2004, in Maeder A., Eenens P., eds, Proc. IAU Symp. 215, Stellar Rotation. Astron. Soc. Pac., San Francisco, p. 168
Fekel F. C., Hinkle K. H., Joyce R. R., Wood P. R., Lebzelter T., 2007, AJ, 133, 17
Friedjung M., Gális R., Hric L., Petrík K., 2003, A&A, 400, 595
Hale A., 1994, AJ, 107, 306
Harries T. J., Howarth I. D., 1996, A&A, 310, 235
Harries T. J., Howarth I. D., 2000, A&A, 361, 139
Hoffleit D., 1970, Inf. Bull. Var. Stars, 469, 1
Hubeny I., Lanz T., Jeffery C. S., 1994, in Jeffery C. S., ed., Newsletter on Analysis of Astronomical Spectra, No. 20, CCP7, St Andrews University, St Andrews, p. 30
Hut P., 1981, A&A, 99, 126
Kaufer A., Stahl O., Tubbesing S., Norregaard P., Avila G., Francois P., Pasquini L., Pizzella A., 1999, The Messenger, 95, 8
Kenyon S. J., 1986, The Symbiotic Stars. Cambridge Univ. Press, Cambridge, New York, p. 295
Kenyon S. J., Fernandez-Castro T., 1987, AJ, 93, 938
Kenyon S. J., Garcia M. R., 1989, AJ, 97, 194
Kenyon S. J., Oliversen N. A., Mikolajewska J., Mikolajewska M., Stencel R. E., Garcia M. R., Anderson C. M., 1991, AJ, 101, 637
Kenyon S. J., Mikolajewska J., 1995, AJ, 110, 391
Kenyon S. J., Mikolajewska J., Mikolajewski M., Polidan R. S., Slovak M. H., 1993, AJ, 106, 1573
Kupka F., Piskunov N. E., Ryabchikova T. A., Stempels H. C., Weiss W. W., 1999, A&AS, 138, 119
Kurucz R. L., 1993, ATLAS9 Stellar Atmosphere Programs (Kurucz CD-ROM 13)
Melo C. H. F., 2003, A&A, 410, 269
Melo C. H. F., Pasquini L., De Medeiros J. R., 2001, A&A, 375, 851
Mikolajewska J., 2003, in Corradi R. L. M. Mikolajewska J., Mahoney T. J., eds., ASP Conf. Ser. Vol. 303, Symbiotic Stars: Probing Stellar Evolution. Astron. Soc. Pac., San Francisco, p. 9
Mikolajewska J., Mikolajewski M., Kenyon S. J., 1989, AJ, 98, 1427
Mikolajewska J., Kenyon S. J., Mikolajewski M., Garcia M. R., Polidan R. S., 1995, AJ, 109, 1289
Mürset U., Schmid H. M., 1999, A&AS, 137, 473
Mürset U., Dumm T., Isenegger S., Nussbaumer H., Schild H., Schmid H. M., Schmutz W., 2000, A&A, 353, 952
Pereira C. B., Vogel M., Nussbaumer H., 1995, A&A, 293, 783
Pucinskas A., 1970, Vilnius Astronomijos Observatorijos Biuletenis, 27, 24
Quiroga C., Mikolajewska J., Brandi E., Ferrer O., García L., 2002, A&A, 387, 139
Schild H., Schmid H. M., 1997, A&A, 324, 606
Schild H., Muerset U., Schmutz W., 1996, A&A, 306, 477
Schmid H. M., Dumm T., Murset U., Nussbaumer H., Schild H., Schmutz W., 1998, A&A, 329, 986
Schild H., Dumm T., Mürset U., Nussbaumer H., Schmid H. M., Schmutz W., 2001, A&A, 366, 972
Schmidt-Kaler T. H., 1982, in Schaifers K., Voigt H. H., eds, Landolt-Brnstein, New Series, Group VI, Vol. 2b, Stars and Star Clusters. Springer-Verlag, New York
Schmutz W., Schild H., Muerset U., Schmid H. M., 1994, A&A, 288, 819
Skopal A., 2005, A&A, 440, 995
Skopal A., Vittone A., Errico L., Bode M. F., Lloyd H. M., Tamura S., 1997, MNRAS, 292, 703
Smith V. V., Cunha K., Jorissen A., Boffin H. M. J., 1997, A&A, 324, 97
Stanishev V., Zamanov R., Tomov N., Marziani P., 2004, A&A, 415, 609
Stawikowski A., 1994, Acta Astron., 44, 393
Tassoul J., 2000, Cambridge Astrophysics Ser. Vol. 36, Stellar Rotation/Jean-Louis Tassoul. Cambridge Univ. Press, Cambridge, New York
Tomov N. A., Tomova M. T., Ivanova A., 2000, A&A, 364, 557
van Belle G. T., Lane B. F., Thompson R. R., Doden A. F., Colavita M. M. et al., 1999, AJ, 117, 521
Yudin B., Munari U., 1993, A&A, 270, 165
Yudin B. F., Shenavrin V. I., Kolotilov E. A., Tatarnikova A. A., Tatarnikov A. M., 2005, Astron. Rep., 49, 232
Yungelson L., Livio M., Tutukov A., Kenyon S. J., 1995, ApJ, 447, 656
Zahn J.-P., 1977, A&A, 57, 383
Zahn J.-P., 1989, A&A, 220, 112

Zamanov R. K., Bode M. F., Melo C. H. F., Porter J., Gomboc A., Konstantinova-Antova R., 2006, MNRAS, 365, 1215 (Paper I)
Zhu Z. X., Friedjung M., Zhao G., Hang H. R., Huang C. C., 1999, A&AS, 140, 69

APPENDIX A: SPECTRA AND CCFS

Here we give a few examples of our spectra (Fig. A1) and graphic representation of the CCF for all SSs observed in this paper (Fig. A2).

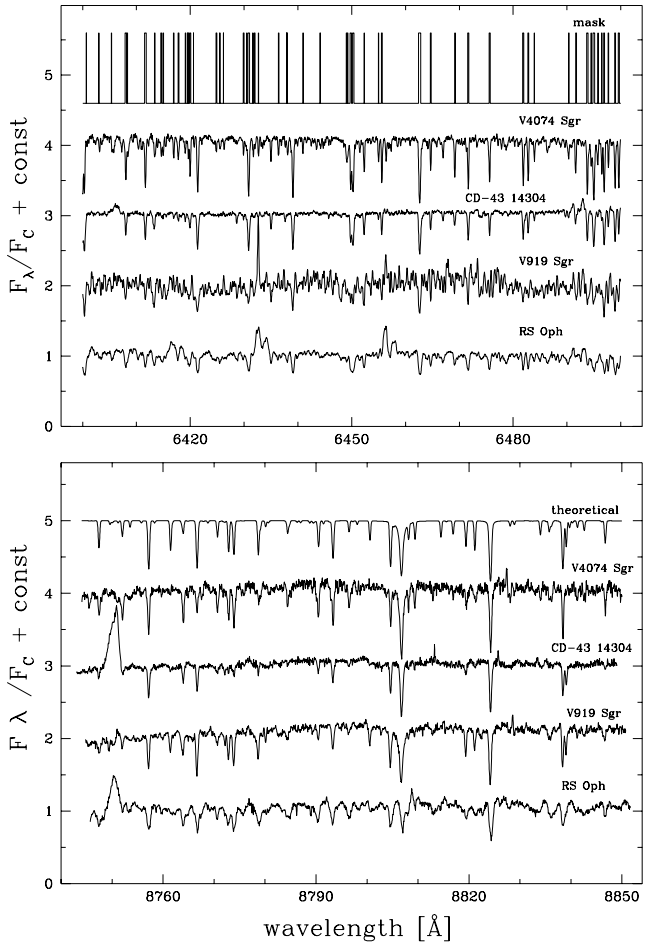

Figure A1. A few examples of our spectra, together with the mask in the interval λλ 6400−6500 Å (upper panel), and with a synthetic spectrum in the interval λλ 8740−8850 Å. The spectra are plotted in increasing order of rotation: V4074 Sgr (M4III, $v \sin i = 3.5$ km s^{-1}), CD-43°14304 (K5III, $v \sin i = 7.2$ km s^{-1}), V919 Sgr (M2III, $v \sin i = 9.1$ km s^{-1}), RS Oph (M0III, $v \sin i = 11.7$ km s^{-1}). The synthetic spectrum corresponds to M0III and $v \sin i = 5$ km s^{-1}.

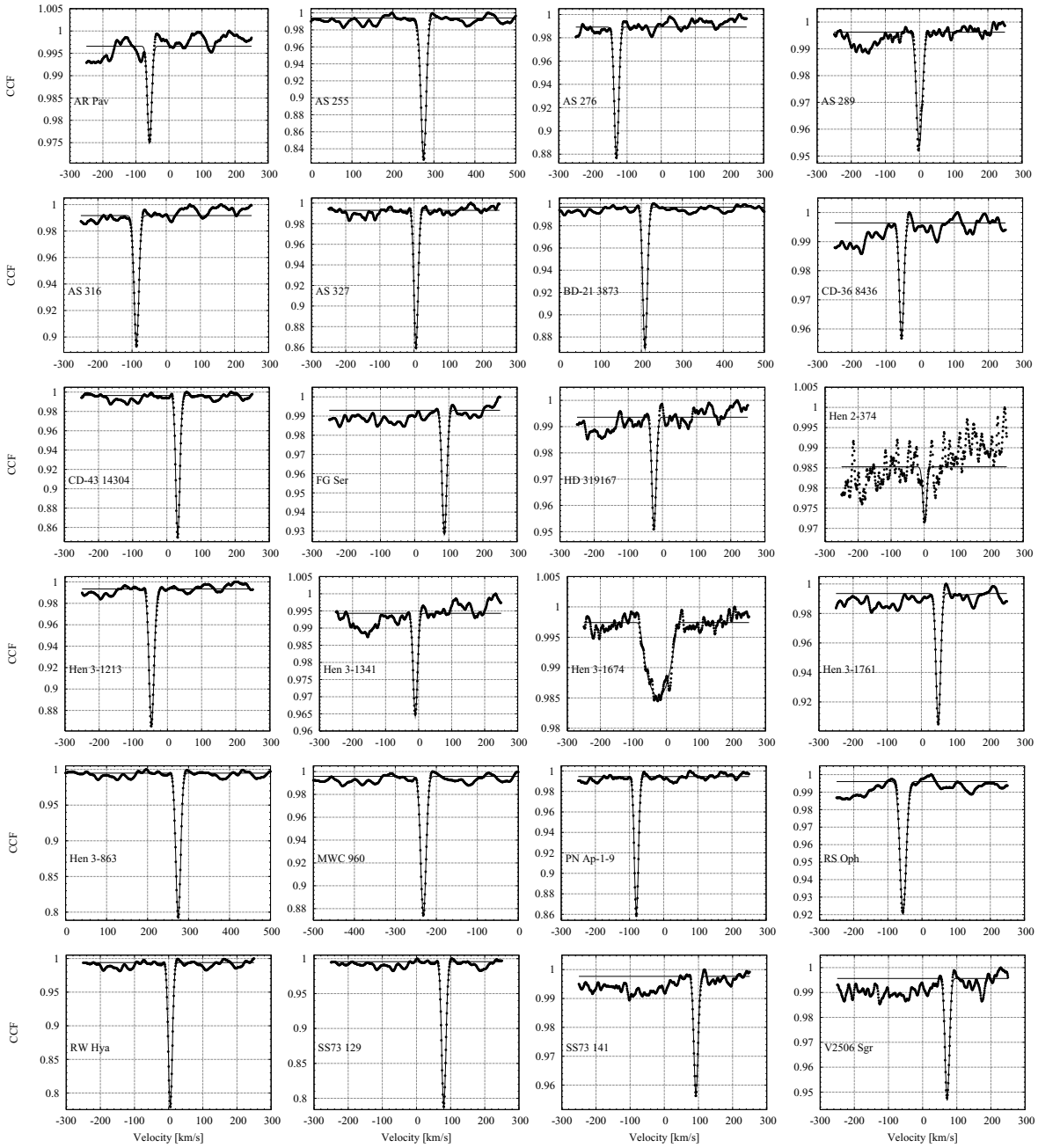

Figure A2. CCF using K0 numerical mask. In each panel are plotted the relative intensity of CCF (heavy line) and the fit versus radial velocity for the SSs observed in this paper. The measured widths of the CCF are given in Table 2.

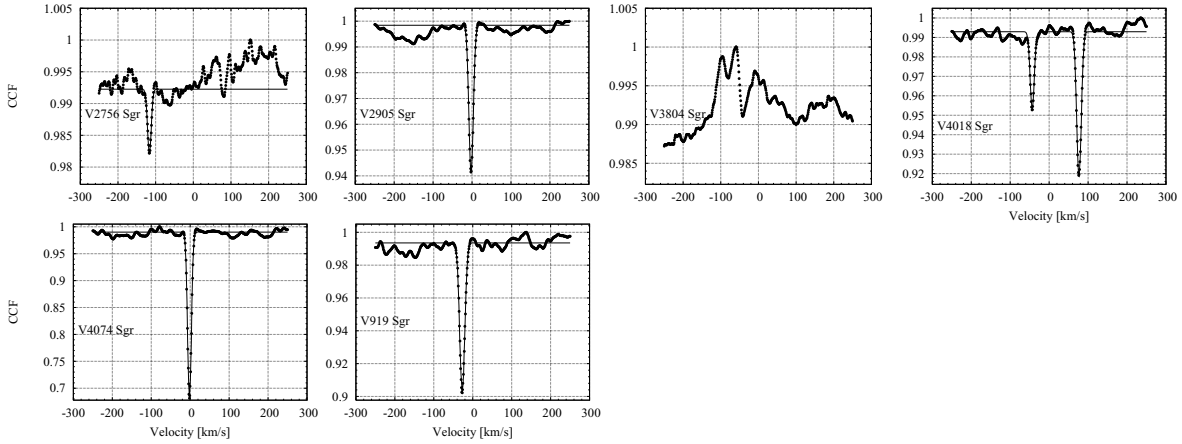

Figure A2 – *continued*

This paper has been typeset from a TEX/LATEX file prepared by the author.